European Journal of Pharmacology 796 (2017) 54–61

Contents lists available at ScienceDirect

European Journal of Pharmacology

journal homepage: www.elsevier.com/locate/ejphar

Behavioural pharmacology

The effect of arsenite on spatial learning: Involvement of autophagy and apoptosis

Behnoosh BonakdarYazdi[a], Fariba Khodagholi[b], Fatemeh Shaerzadeh[c], Azadeh Sharifzadeh[d], Ramesh Ahmadi[d], Mehdi Sanati[a], Hajar Mehdizadeh[a,e], Borna Payandehmehr[a], Leila Vali[f], Mehrnoush Moghaddasi Jahromi[g], Ghorban Taghizadeh[a,e,h], Mohammad Sharifzadeh[a,e,*]

[a] Department of Pharmacology and Toxicology, Faculty of Pharmacy, Toxicology and poisoning Research Centre, Tehran University of Medical Sciences, Tehran, Iran
[b] Neuroscience Research Center, Shahid Beheshti University of Medical Sciences, Tehran, Iran
[c] Department of Physiology, faculty of medicine, Hormozgan University of Medical Sciences, Bandar Abbas, Iran
[d] Department of Physiology, Azad University, Qom, Iran
[e] Department of Neuroscience, School of Advanced Technologies in Medicine, Tehran University of Medical Sciences, Tehran, Iran
[f] Department of Medical Laboratory Sciences, Faculty of Allied Health Sciences, Kuwait University, Sulaibekhat, Kuwait
[g] Physiology Department, School of Medicine, Lorestan University of Medical Sciences, Khoramabad, Iran
[h] Department of Occupational Therapy, Faculty of Rehabilitation Sciences, Iran University of Medical Sciences, Tehran, Iran

ARTICLE INFO

Keywords:
Sodium arsenite
Autophagy
Apoptosis
Alzheimer disease
Spatial learning
Caspase-3
LC3

ABSTRACT

Spatial learning plays a major role in one's information recording. Arsenic is one of ubiquitous environmental toxins with known neurological effects. However, studies investigating the effects of arsenic on spatial learning and related mechanisms are limited. This study was planned toexaminethe effects of bilateral intra-hippocampal infusion of different concentrations of sodium arsenite (5, 10 and 100 nM, 5 μl/side) on spatial learning in Wistar rats. Moreover, we evaluated levels of LC3-II, Atg7 and Atg12 as reliable biomarkers of autophagy and caspase-3 and Bax/Bcl-2 ratio as indicators of apoptosis in the hippocampus. Interestingly, low concentrations of sodium arsenite (5 and 10 nM) significantly increased spatial acquisition but pre-training administration of sodium arsenite100 nM did not significantly alter spatial learning. LC3-II levels were significantly increased in groups treated with sodium arsenite 5 and 10 nM and decreased in the group receiving arsenite 100 nM compared to the control group. Atg7 and Atg12 levels were obviously higher in all groups treated with sodium arsenite compared to control. However, caspase-3 cleavage and Bax/Bcl-2 ratio were notably greater in 100 nM, and lesser in 5 nM arsenite group in comparison with control animals.

The results of this study showed that the low concentrations of sodium arsenite could facilitate spatial learning. This facilitation could be attributed to neuronal autophagy induced by low concentrations of sodium arsenite. These findings may help to clarify the regulatory pathways for apoptosis and autophagy balance due to sodium arsenite.

1. Introduction

Arsenic is one of the environmental toxicants ubiquitously found in water, air and soil. The primary source of human exposure is through drinking contaminated water (Martinez-Finley et al., 2009). Arsenic and its derivatives are thoroughly studied for their carcinogenic effects focusing on increased risk of skin, bladder, liver and kidney tumors (Diaz-Villasenor et al., 2006). In 2003, Rodriguez et al. reviewed the effects of arsenic on nervous system, declaring adverse effects of arsenic on neurobehavioral development (Rodriguez et al., 2003). Deficits in learning and memory following acute or chronic arsenic exposure have been reported in many human and animal studies. However, their cellular and molecular mechanisms are not understood completely (O'Bryant et al., 2011; Tsai et al., 2003). Luo et al. (2009) reported that long-term exposure to high concentration of arsenic in drinking water resulted in significant delay in acquisition of spatial memory but it had not significant effect on spatial memory retention (Luo et al., 2009). On the other hand, Jiang et al. (2014) and Jing et al. (2012) indicated impairment of both acquisition and retention of spatial memory due to long-term exposure to high dose of arsenic

* Corresponding author at: Department of Pharmacology and Toxicology, Faculty of Pharmacy, Tehran University of Medical Sciences, Tehran, Iran.
E-mail address: msharifzadeh@sina.tums.ac.ir (M. Sharifzadeh).

http://dx.doi.org/10.1016/j.ejphar.2016.12.023
Received 20 April 2016; Received in revised form 3 December 2016; Accepted 15 December 2016
Available online 18 December 2016

(Jiang et al., 2014; Jing et al., 2012). Then again, our recent study showed the dual effect of sodium arsenite on contextual and tone memory of Aβ-injected rats in pavlovian fear conditioning model. We found that low dose (1 and 5 nM) of sodium arsenite attenuated memory deficit induced by amyloid beta while high dose (10 and 100 nM) increased memory loss in these rats. Arsenite at these ultra-low concentrations caused a marked increase in Nrf2 and CREB phosphorylation and a significant decrease in caspase-3 and NF-κB amount (Nassireslami et al., 2016). This dual effect of sodium arsenite may be observed in spatial learning; however, it has not yet been studied. Additionally, low doses of arsenite undergo enzymatic methylation in the liver to the extent of 80% after oral administration (Vahter, 1981). It is worth mentioning that methylated arsenicals excreted more rapidly than inorganic arsenic in the urine (Rodriguez et al., 2001). Moreover methylated and inorganic arsenite have different effects on neuronal cells. It has been reported that in contrast to arsenite, methylated arsenicals did not cover cell viability of astrocytes (Dringen et al., 2016). So, regarding to the above description and the properties of low dose of sodium arsenite, we aimed at investigating the effects of local and direct intra-hippocampal injection of low and high doses of sodium arsenite on spatial memory.

Furthermore, it has been previously reported that sodium arsenite could induce both autophagic and apoptotic responses (Bolt et al., 2010, 2012; Keim et al., 2012). Autophagy and apoptosis are two major types of programmed cell death that are main mechanisms for cells survival (Salminen et al., 2013). Apoptosis, a process triggering a signaling cascade to definitive cellular death, have been thoroughly investigated and it is established that two protein families are involved in its regulation: B lymphoma 2 (Bcl-2) family members and cysteine-aspartic acid protease (caspase) family (Bolt et al., 2010; D'Amelio et al., 2012; Shin et al., 2011). Autophagy is considered as an evolutionarily cell survival process, which is responsible for degradation of long-lived proteins and removal of dysfunctional organelles (Ding et al., 2013). There are many pathways involved in the process of autophagosomes formation, fusion with lysosomes to form lysosomic vacuoles (i.e. autolysosomes) and their degradation (Yue et al., 2009). Two ubiquitin-like pathways are important in forming autophagic vesicle. The first is covalent conjugation of Atg12 and Atg5 by E1 ligase-like protein Atg7 which is essentially needed for progression of the second pathway that is conjugation of long chain 3 (LC3) protein to a phospholipid molecule leading to expansion of autophagic membrane. This conjugate converts soluble LC3-I to autophagic vesicle-associated LC3-II (Gozuacik and Kimchi, 2007). Measuring the conversion of LC3-I to LC3-II helps to quantify autophagic activity (Mizushima and Yoshimori, 2007).

It seems that autophagy and apoptosis function appositely. While apoptosis is a cellular suicidal program, autophagy can either be a cell survival mechanism as a homeostatic process or a stress-induced cell death pathway depending on variable context (Bolt et al., 2010; Kralova et al., 2012).

Therefore, in search for crosstalk between apoptosis and autophagy pathways and to see how sodium arsenite affects these processes, the levels of Bax, Bcl-2 and caspase-3, as major markers involved in apoptosis, and also LC3, Atg7 and Atg12, as major proteins playing important roles in autophagy, were assessed. The main purpose of our study was a better understanding of the local and direct effects of sodium arsenite on spatial learning and determining its related mechanisms in the brain.

2. Material and methods

2.1. Materials

Antibodies directed against Caspase-3, LC3, Bax, Bcl-2, Atg7, Atg12 and β-actin were purchased from Cell Signaling Technology (Beverly, MA, USA). Electrochemiluminescence (ECL) kit was obtained from Amersham Bioscience (Piscataway, NJ, USA). Sodium arsenite and all other reagents were purchased from Sigma Aldrich (St. Louis, MO, USA).

2.2. Animals

Male Wistar Rats (220 ± 20 g) were purchased from the animal house of the Tehran University of Medical Sciences. All animals were housed in cages (four/cage) with ad libitum access to food and water. They were kept on a 12 h-light/dark cycle at a constant temperature (20–22 °C). All animal experiments were performed in daylight and according to the guidelines of the Ethical Committee for the Care and Use of Laboratory Animals of Tehran University of Medical Sciences (code: 23516-151-02-92, 2013). All efforts were made to minimize animal suffering and to reduce the number of animals used.

2.3. Stereotaxic surgery

Under anesthesia with intraperitoneal injection of 100 mg/kg ketamine and 25 mg/kg xylazine, animals were placed into stereotaxic apparatus (Stoelting, Wood Dale, IL, USA). Stereotaxic coordinates used for intra-hippocampal injection according to the atlas of Paxinos and Watson, were as follows: Anterior–posterior (AP), 3.8 mm posterior to the bregma; medial-lateral (ML), ± 2.2 mm lateral to the sagittal suture and dorsal–ventral (DV), 2.7 mm down from the skull surface. Guide cannulas (21-gauge) were inserted bilaterally into the dorsal hippocampus (CA1 region) and were attached to the skull surface using orthopedic cement (synment®). After cannulation, animals were maintained in their cages and handled daily for one week as a recovery period. Microinjection was performed using a 10 μl Hamilton microsyringe and an injection needle (27-gauge) attached to polyethylene tube (PE-10) 30 min before each training session.

2.4. Experimental design

In the present study, animals were assigned into four groups. All animals of these four groups underwent stereotaxic surgery and cannula implantation. Different concentrations of sodium arsenite (5, 10, 100 nM) were infused bilaterally (5 μl/side) via intra-hippocampal cannula. Control group received 5 μl/side normal saline via intra-hippocampal injection. Animals were trained for four consecutive days and all injections were made 30 min before training.

2.5. Behavioral tests

Morris water maze (MWM) includes a black-painted circular pool (136 cm diameter, 60 cm height), divided into four equal quadrants. A platform made of Plexiglas was located in north-west quadrant (target quadrant) and tank was filled with water (25 ± 2 °C) up to 1 cm above surface of platform. After 1 week recovery period of surgery, training was done for 4 consecutive days. One block of 4 trials was conducted on each day. Each trial was started with placing animals in one of starting points (north, east, south and west) of MWM. Animals were let to swim freely for 90 s to find the immersed platform. If a rat did not find the platform, it was manually guided to platform. Animals were allowed to rest 30 s between two trials. Directions of rats were recorded by a video camera linked to a computer, located above MWM center. Spatial learning and memory parameters were evaluated using EthoVision video tracking system (Noldus Information Technology, Wageningen, Netherlands). Escape latency (time to find the hidden platform), traveled distance (path length to reach the hidden platform), and swimming speed were measured for further analyses. Probe test was conducted on day 5 to evaluate time spent in target quadrant and hidden platform's proximities. In probe test, hidden platform was removed; all animals were placed in the same starting point opposite of target quadrant and allowed to swim for 90 s. The visible test was

conducted to assess motivation and visuo-motor coordination. Visible platform test included groups of independent animals with the same treatment profile and training trials. In this test, platform was elevated above water level in the center of opposite quadrant of previously hidden platform and covered with aluminum foil. Details for MWM test were thoroughly described in our previous studies (Azami et al., 2012; Khorshidahmad et al., 2012; Sharifzadeh et al., 2005).

2.6. Western blotting

When probe test was done, rats were euthanized in a CO_2 chamber immediately and the hippocampus was bilaterally dissected. Using lyses buffer containing sodium deoxycholate 0.5%, NaCl 150 mmol/l, SDS 0.1%, EDTA 100 mmol/l, Triton X100 1% and protease inhibitor cocktail with pH of 7.4, brain tissues were homogenized and then centrifuged for 5 min at 12,000×g at 4 °C in a micro centrifuge three times and supernatant was collected eventually. In order to measure total protein concentrations, Bradford assay was used (Bradford, 1976). All samples' concentrations were calculated using a standard curve generated for bovine serum albumin. Samples were frozen at −20 °C for later use. After gel preparation, 60 µg of total protein sample along with sample buffer and water was loaded onto the gel (12 µl per well). Proteins were electrophoretically separated in 12% SDS-PAGE gels and were transferred to polyvinylidene fluoride (PVDF) membrane. Blocking of any remaining sites on PVDF membrane was done by incubating membrane in skimmed milk 5% for 75 min. Afterwards, primary antibody was added and membrane was incubated overnight to probe with the specific protein. A HRP enzyme conjugated secondary antibody, at a species-specific portion of the primary antibody, was used and the membrane was incubated for another 75 min. Immunoreactive polypeptides were visualized by chemiluminescence using enhanced ECL reagents and the location of the protein bands was revealed. Subsequently, X-ray films were exposed to the membrane in a dark room and using developer and fixer solutions visible images were made. Densitometrical measurements were carried out using ImageJ 1.410 software (NIH, USA). All bands were normalized to β-actin (Hosseini-Sharifabad et al., 2011).

2.7. Statistical analysis

An average value for each memory parameter (escape latency, traveled distance, and swimming speed) was calculated over four trials in four days of training. Comparison of behavioral (time spent in target quadrant and proximity and swimming speed in probe test as well as mean of escape latency, traveled distance, and swimming speed in training days) and molecular data were done using One-way analysis of variance (ANOVA). A mixed between-within subjects analysis of variance was conducted to assess the impact of treatment groups (4 factor) on escape latency, traveled distance, and swimming speed across four training days (4 factor). The Bonferroni's multiple comparison post hoc test was selected and used to analyze differences between groups. A P-value < 0.05 was defined as statistically significant.

3. Results

3.1. Sodium arsenite: Spatial learning and memory's friend or foe?

3.1.1. Low concentrations of sodium arsenite enhanced acquisition of spatial memory in MVM

Mean of escape latency (s), traveled distance (cm) and swimming speed (cm/s) for a four-day training program after intra-hippocampal infusion of different concentrations of sodium arsenite is shown in Fig. 1. There was a statistically significant difference in both mean of escape latency ($F_{(3, 24)}=14.20$, $P < 0.0001$) and traveled distance (treatment groups: $F_{(3, 24)}=15.50$, $P < 0.0001$) for the four treatment groups. However, a significant difference in swimming speed ($F_{(3, 24)}=0.21$, $P=0.89$) was not observed in the treated animals. Rats receiving 5 and 10 nM of sodium arsenite showed significant decrease in both escape latency and traveled distance compared to either control or group of 100 nM sodium arsenite infusions (Fig. 1A, B, respectively). No significant differences were seen in swimming speed among all groups of animals ($P > 0.05$) (Fig. 1c).

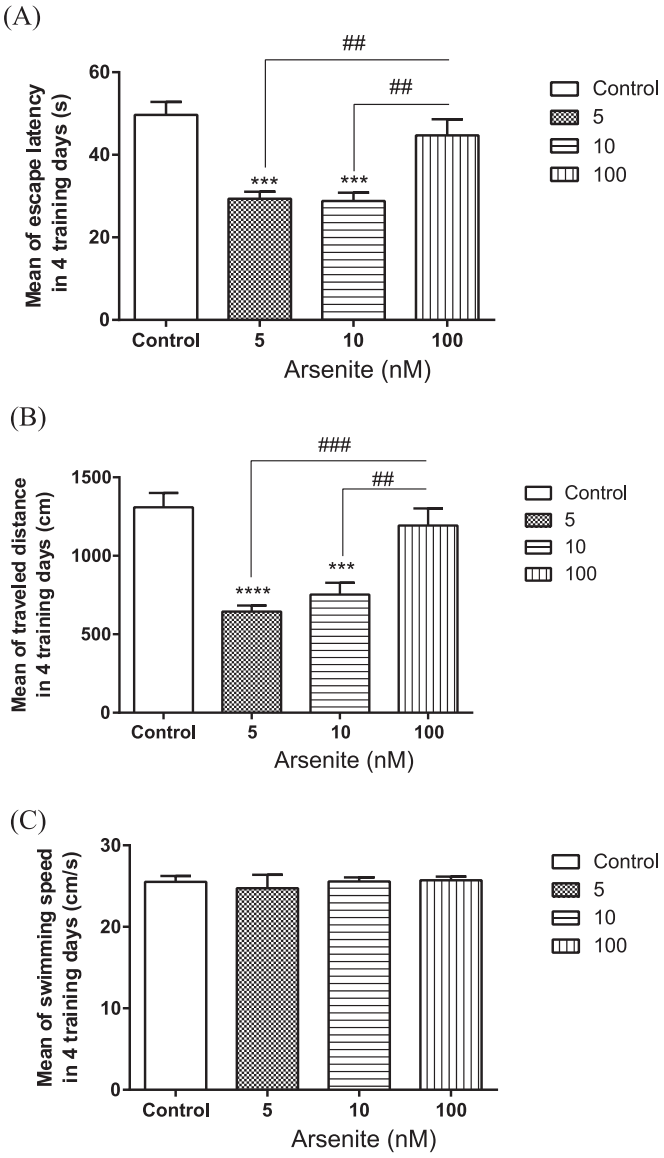

Fig. 1. Mean of escape latency (A), traveled distance (B) and swimming speed (C) during four training days in the morris water maze task. ***P < 0.001 and ****P < 0.0001 compared to control group. ##P < 0.01 and ###P < 0.001 indicates compared to the Arsenite 100 nM group. Data are presented as means ± S.E.M and n =7 animals serve as subjects in each group.

The main effects of treatment groups and training days were significant for both escape latency (treatment groups: $F_{(3, 24)}=14.20$, $P < 0.0001$; training days: $F_{(3, 72)}=58.08$, $P < 0.0001$) and traveled distance (treatment groups: $F_{(3, 24)}=15.50$, $P < 0.0001$; training days: $F_{(3, 72)}=40.65$, $P < 0.0001$) while the interaction effect of treatment groups by training days was not significant for any of these measures (escape latency: $F_{(9, 72)}=0.59$, $P=0.8$; traveled distance: $F_{(9, 72)}=1.61$, $P=0.13$) (Fig. 3A and B). The main effects of treatment groups ($F_{(3, 24)}=0.21$, $P=0.89$), training days ($F_{(3, 72)}=1.71$, $P=0.17$) and the interaction effect of treatment groups by training days ($F_{(9, 72)}=0.45$, $P=0.90$) were not significant for swimming speed (Fig. 3C). Statistical comparison of different concentrations of sodium arsenite, considering the same training days, shows that administration of sodium arsenite

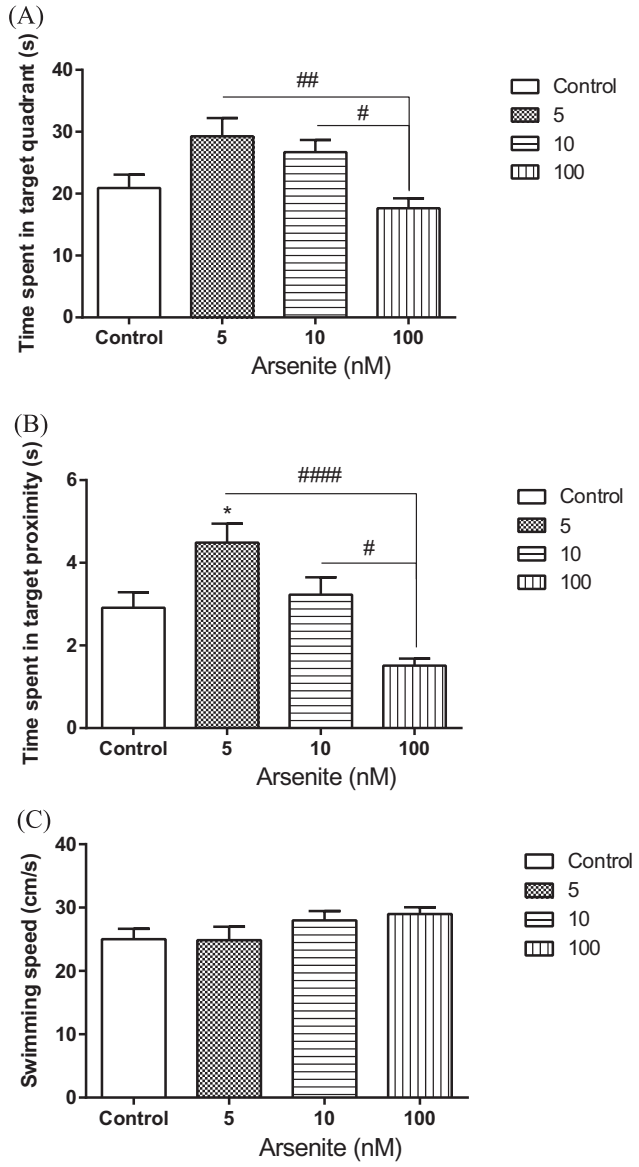

Fig. 2. Time spent in target quadrant (A), Time spent in target proximity (B) and swimming speed (C) in probe test after four days of training in morris water maze task. *P < 0.05 compared to control group. #P < 0.05, ##P < 0.01, ####P < 0.0001 compared to the Arsenite 100 nM group. There were no significant differences in swimming speed (P > 0.05). Data are presented as means ± S.E.M and n =7 animals serve as subjects in each group.

(5 nM, 5 μl/side) may lead to significant decrease in escape latency on both day1 (P < 0.05) and day 2 (P < 0.0001) compared to control group. It also caused memory improvement via decreasing traveled distance (cm) on the second (P < 0.0001), third (P < 0.05) and fourth (P < 0.01) days. In addition, sodium arsenite (10 nM) led to a significant decrease in escape latency (s) and traveled distance (cm) on second and third days of training compared to control group. Escape latency (s) was increased significantly by sodium arsenite (100 nM) on day 2 (P < 0.05) compared to 5 nM group and also on day 2 and 3 (P < 0.05 for both days) in comparison with 10 nM treated rats. Sodium arsenite (100 nM, 5 μl/side) also significantly increased traveled distance (cm) on day 2 (P < 0.01), 3 (P < 0.05) and 4 (P < 0.05) compared to group received sodium arsenite 5 nM. Also, Sodium arsenite (100 nM, 5 μl/side) meaningfully increased traveled distance (cm) on day 2 and 3 (P < 0.05 for both days) compared to group received sodium arsenite 10 nM. Multiple comparisons did not show any significant difference in swimming speed between different groups.

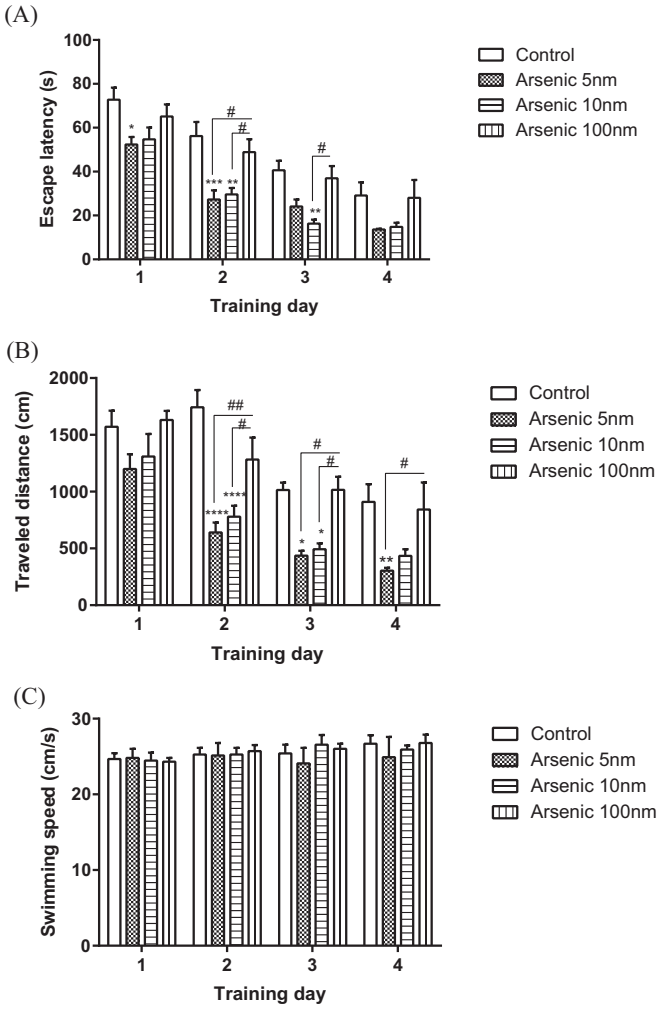

Fig. 3. Evaluation and comparison of escape latency (A), traveled distance (B) and swimming speed (C) on the same training day in arsenite treated animals. The figure shows significant changes in escape latency and traveled distance *P < 0.05, **P < 0.01, ***P < 0.001 and ****P < 0.0001 compared to control group and #P < 0.05 and ##P < 0.01 compared to the Arsenite 100 nM group. Data are presented as means ± S.E.M of 7 animals in each group.

3.1.2. Different concentrations of sodium arsenite could have different effects on rat's performance in probe test

After completing 4 days training, probe test was done on fifth day. There was a statistically significant difference in both time spent in target quadrant ($F_{(3, 24)}$=5.70, P=0.004) and time spent in target proximity ($F_{(3, 24)}$=10.75, P=0.0001) in probe test for the four treatment groups. However, a significant difference in swimming speed was not detected ($F_{(3, 24)}$=1.66, P=0.20) in probe test among four treatment groups. Our results showed that bilateral injection of sodium arsenite (5 nM) could significantly increase time spent in platform's proximity during 90 s of probe test compared to control group. Furthermore, bilateral injection of sodium arsenite 100 nM significantly decreased time spent in target quadrant and platform's proximity in comparison to the group receiving sodium arsenite 5 nM and 10 nM. Swimming speed was not significantly different among all groups of animals (Fig. 2a-c).

3.2. Sodium Arsenite and Apoptosis

3.2.1. Effects of sodium arsenite on Bax/Bcl-2ratio in hippocampus of rats

There was a significant difference in Bax/Bcl-2 ratio ($F_{(3, 8)}$ =1756, P < 0.0001) in four treatment groups. As shown in Fig. 4, Bax/Bcl-2

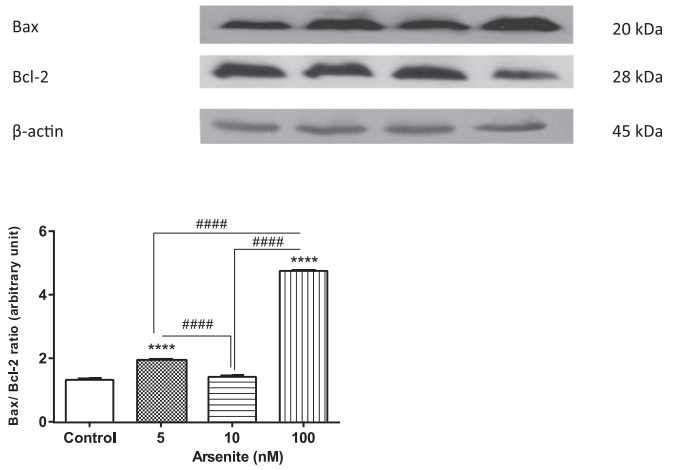

Fig. 4. The effect of sodium arsenite on Bax/Bcl-2 ratio in the hippocampus of arsenite treated rats 5 days after injection. One representative Western blot is shown (n=7). The densities of Bcl-2 and Bax bands were measured and the ratio to the β-actin bands was calculated. Each point shows the mean ± S.E.M. ****P < 0.0001 significant difference compared to the vehicle group, ####P < 0.0001 significant difference between arsenite groups.

ratio increased by sodium arsenite 100 nM and 5 nM compared to control group. This ratio was significantly lower in sodium arsenite 5 nM and 10 nM groups compared to 100 nM treated animals.

3.2.2. Effects of sodium arsenite on caspase-3 cleavage in hippocampus of rats

A significant difference in cleavage of caspase-3 ($F_{(3, 8)}$=123.6, P < 0.0001) was observed in treated groups. As the major indicator of apoptosis, cleavage of caspase-3 was assessed by western blotting in our study. As shown in Fig. 5, cleaved caspase-3 level was significantly lower and higher in 5 nM and 100 nM sodium arsenite treated animals in comparison with control group, respectively. The cleavage of caspase-3 was significantly lesser in groups of 5 nM and 10 nM sodium arsenite compared to 100 nM administration.

3.3. Sodium Arsenite and Autophagy

3.3.1. Effects of sodium arsenite on autophagic markers in hippocampus of rats

In this study, we used western blot to analyze different proteins involved in autophagy. LC3-I converts to LC3-II, the phpsopholipid-

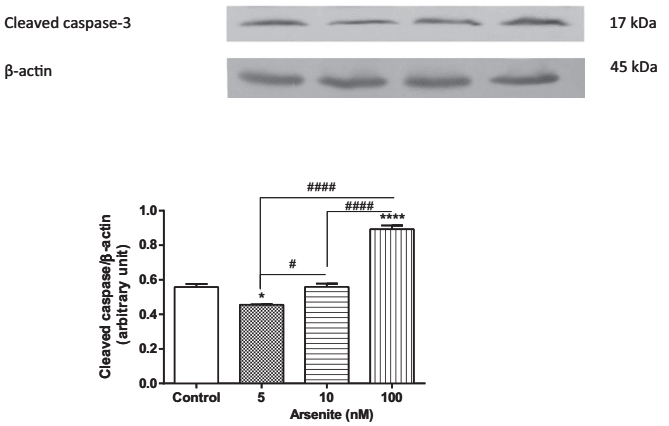

Fig. 5. The effect of sodium arsenite on the cleavage of caspase-3 in the hippocampus of arsenite treated rats 5 days after injection. One representative Western blot is shown (n=7). The densities of caspase-3 bands were measured and the ratio to the β-actin bands was calculated. Each point shows the mean ± S.E.M. ****P < 0.0001 significant difference compared to the vehicle group, #P < 0.05 and ####P < 0.0001 significant difference between arsenite groups.

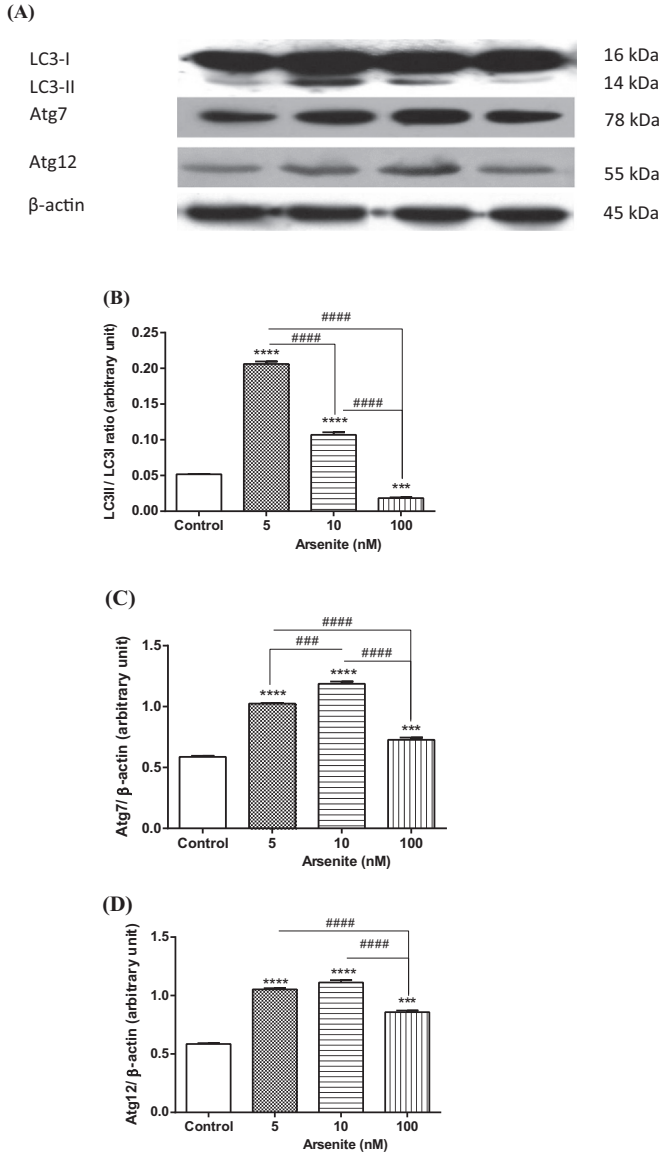

Fig. 6. The effect of sodium arsenite on (B) LC3 conversion, (C) Atg7 and (D) Atg12 protein level in the hippocampus of arsenite treated rats 5 days after injection. (A) One representative Western blot is shown (n=7). The densities of LC3-I, LC3-II, Atg7 and Atg12 bands were measured and the ratio of LC3-II to LC3-I and Atg7 and Atg12 to the β-actin bands was calculated. Each point shows the mean ± S.E.M. ***P < 0.001 and ***P < 0.0001 significant difference compared to the vehicle group, ####P < 0.0001 significant difference between arsenite groups.

linked form, indicating presence of autophagolysosomes in groups receiving sodium arsenite 5 and 10 nM. There was a statistically significant difference in LC3-II/LC3-I ratio ($F_{(3, 8)}$ =997.90, P < 0.0001) for the four treatment groups. The LC3-II/LC3-I ratio was significantly increased in 5 nM and 10 nM sodium arsenite groups and decreased in 100 nM sodium arsenite infused rats compared to control group. The LC3-II/LC3-I ratio was significantly higher in sodium arsenite 5 nM and 10 nM groups in comparison with 100 nM treated group (Fig. 6B).

Atg7 and Atg12 were two other autophagy related proteins analyzed by western blotting in our experiment. There was a statistically significant difference in both Atg7 ($F_{(3, 8)}$=386, P < 0.0001) and Atg12 ($F_{(3, 8)}$=295.6, P < 0.0001) levels for the four treatment groups. Our results evidently showed that in all sodium arsenite treated groups, Atg7 and Atg12 levels were increased compared to control group. But these markers were also significantly reduced in sodium arsenite 100 nM group compared to other arsenite treated groups (Fig. 6C

and D).

4. Discussion

The present study was designed to determine the effects of sodium arsenite on spatial learning as well as autophagy and apoptosis. Our findings showed that intra-hippocampal injection of arsenite with low concentrations (5, 10 nM/side) can improve spatial learning in a four-day training program in MWM. Besides, there's a progression in rats' performance in probe test for 5 nM sodium arsenite group. However, high concentration of arsenite (100 nM/side) did not alter the spatial learning and memory parameters in MWM performance, directing us to conclude that different concentrations of arsenite may operate through different pathways and result in different behavioral outcomes. Like many other toxicants, neurobehavioral alterations after arsenic exposure is affected by several intervening variables among which are the concentration and duration of exposure, along with experimental conditions (Komissarova et al., 2005; Rodriguez et al., 2001). For many years, arsenic has been studied for its toxic effects. It has been associated with many health conditions like neurobehavioral deficits and cancer. There are also reports in which it was associated with cell proliferation and anti-cancer effects. The mechanisms underlying this controversy remain unclear (Ratnaike, 2003; Simeonova et al., 2000). Although arsenic is a well-known neurotoxicant which affects CNS by inducing apoptosis, oxidative stress and neuronal cell death, many pathways have been reported as proposed mechanisms for low arsenite concentration-induced cell proliferation (Chan and Huff, 1997; Chowdhury et al., 2010; He et al., 2007; Luster and Simeonova, 2004; Watcharasit et al., 2012).

In search for underlying mechanisms, we applied western blotting to see how apoptotic and autophagic molecular markers would be affected by sodium arsenite. Our results elucidated that high concentration of arsenite can trigger apoptosis through increasing Bax/Bcl-2 ratio followed by caspase-3 activation, while low concentration of arsenite is more involved in processes related to autophagy. Interestingly, 10 nM concentration of sodium arsenite showed dual effect on Bax and Bcl-2 protein levels. Whilst Bcl-2 level in 10 nM arsenite-injected rats was near to control and low concentration of arsenite, Bax level considerably decreased in this group. This dual effect of arsenic could be attributed to biphasic dose-response relationship of arsenic on Bax conformational changes and oligomerization. Sodium arsenite is a derivative of arsenic, a semimetal element, capable of chemically interacting with different biological molecules and enzymes via cysteine residues and thus can influence many cellular pathways (Delnomdedieu et al., 1994). Biphasic effect of arsenite on either cell proliferation or apoptosis was also previously suggested (He et al., 2007; Qian et al., 2007) and it seems that different pathways and molecules are involved in regulation of this dual consequence.

First and foremost, arsenic is involved in reactive oxygen species (ROS) production (Druwe and Vaillancourt, 2010; Lau et al., 2013a). It has been suggested that arsenite-induced ROS formation may happen by inhibition of reductase enzymes involved in arsenite oxidation of Fenton reaction in the presence of Fe^{2+}. Arsenite-induced cellular toxicity can also lead to ROS production (Hughes et al., 2011). It has been shown that arsenic causes ROS production in a concentration-dependent manner (Druwe and Vaillancourt, 2010; Eblin et al., 2008; Yang et al., 2007). High-concentration of arsenite increases cellular ROS level, but lower concentrations reduce ROS production (Lau et al., 2013b). ROS can contribute to both apoptosis and autophagy. Chen et al. have suggested that arsenite-induced apoptosis is due to hydrogen peroxide synthesis. Arsenite activates NADPH oxidase which results in higher superoxide level that consequently converts to hydrogen peroxide by Superoxide Dismutase (SOD) (Chen et al., 1998). Accordingly, hydrogen peroxide induces cytochrome C release, activates caspase 3 and lastly stimulates cellular apoptosis (Chen et al., 1998; Taghizadeh et al., 2016). Hydrogen peroxide could also down regulate Bcl-2 by oxidation of cysteine residue and therefore triggers apoptosis (Li et al., 2004; Luanpitpong et al., 2013). Caspase 3 activation further cleaves cAMP response element binding protein (CREB) (Francois et al., 2000) which is crucial for memory formation (Matsuzaki et al., 2006; Mizuno et al., 2002; Williams et al., 2008). In other words, high concentration of sodium arsenite may impair learning and memory due to caspase 3-induced CREB cleavage.

On the other hand, ROS can commence autophagic pathway too. ROS is able to up-regulate Beclin1, oxidize cysteine residues in Atg4 and provokes expression of Atg7 (Chen et al., 2008; Gibson, 2010; Scherz-Shouval et al., 2007; Trejo-Solís et al., 2012). Furthermore, it has been shown that autophagy induced by lower concentrations of arsenite can be initiated by activating Nrf2 pathways, regardless of ROS (Lau et al., 2013b). Previous studies have provided indirect evidences about the role of autophagy enhancement in memory improvement (Caccamo et al., 2010; Carloni et al., 2010), therefore memory enhancement induced by low concentration of sodium arsenite in the current study could be in part related to the increased autophagy.

The results of the current study indicated that high concentration of arsenite increased apoptosis (i.e., cleaved caspase-3 and Bax) and decreases autophagic markers (i.e., Atg7, Atg12 and LC3-II) compared to lower concentration of arsenite. Consistent with our results, it has been previously shown that caspase, by cleaving and inactivating of Beclin-1, can inhibit Becline-1 mediated autophagic effects (Djavaheri-Mergny et al., 2010; Kang et al., 2011; Wirawan et al., 2010). Noteworthy, caspase-mediated Atg4D cleavage can also regulate autophagy. Cleaved Atg4D is highly toxic and triggers apoptosis (Betin and Lane, 2009; Jain et al., 2013).

In addition, the current study found that Bcl-2 level was higher in group treated with low concentration of arsenite in comparison to higher concentration groups putting weight to autophagic side of apoptosis-autophagy balance. Bcl-2 can adjoin Beclin-1 and block Beclin-1 related autophagy (Cho et al., 2009; Pattingre et al., 2005; Thorburn, 2008). Moreover, it is an apoptosis-blocking oncogene (Yousefi and Simon, 2007).

In conclusion, the results of this study showed that bilateral intra-hippocampal injection of lower concentration of sodium arsenite facilitated the acquisition of spatial learning. Furthermore, the current study found that arsenite in low concentrations enhanced autophagy and diminished apoptosis while the higher concentrations of arsenite showed opposite effects. Although our study has not established a causal relationship between underlying mechanisms for memory alteration and sodium arsenite administration, the facilitation of spatial memory due to low concentration of sodium arsenite could be attributed to arsenite-induced neuronal autophagy.

Conflict of interest

The authors declare no conflict of interest.

Acknowledgments

This work was supported by funds (No. 92-02-33-23268) from the Tehran University of Medical Sciences (TUMS) and Lorestan University of Medical Sciences (No. 1283). We thank Dr. Kian Azami and Dr. Ali Hosseini for their generous scientific advices and Mr. Ali Kazemi and Mr. Mehdi Gholami for their technical assistance.

References

Azami, K., Tabrizian, K., Hosseini, R., Seyedabadi, M., Shariatpanahi, M., Noorbakhsh, F., Kebriaeezadeh, A., Ostad, S.N., Sharifzadeh, M., 2012. Nicotine attenuates spatial learning deficits induced by sodium metavanadate. Neurotoxicology 33, 44–52.

Betin, V.M., Lane, J.D., 2009. Caspase cleavage of Atg4D stimulates GABARAP-L1 processing and triggers mitochondrial targeting and apoptosis. J. Cell Sci. 122, 2554–2566.

Bolt, A.M., Byrd, R.M., Klimecki, W.T., 2010. Autophagy is the predominant process

induced by arsenite in human lymphoblastoid cell lines. Toxicol. Appl. Pharmacol. 244, 366–373.
Bolt, A.M., Zhao, F., Pacheco, S., Klimecki, W.T., 2012. Arsenite-induced autophagy is associated with proteotoxicity in human lymphoblastoid cells. Toxicol. Appl. Pharmacol. 264, 255–261.
Bradford, M.M., 1976. A rapid and sensitive method for the quantitation of microgram quantities of protein utilizing the principle of protein-dye binding. Anal. Biochem. 72, 248–254.
Caccamo, A., Majumder, S., Richardson, A., Strong, R., Oddo, S., 2010. Molecular interplay between mammalian target of rapamycin (mTOR), amyloid-beta, and Tau: effects on cognitive impairments. J. Biol. Chem. 285, 13107–13120.
Carloni, S., Girelli, S., Scopa, C., Buonocore, G., Longini, M., Balduini, W., 2010. Activation of autophagy and Akt/CREB signaling play an equivalent role in the neuroprotective effect of rapamycin in neonatal hypoxia-ischemia. Autophagy 6, 366–377.
Chan, P.C., Huff, J., 1997. Arsenic carcinogenesis in animals and in humans: mechanistic, experimental, and epidemiological evidence. J. Environ. Sci. Health Part C 15, 83–122.
Chen, Y., McMillan-Ward, E., Kong, J., Israels, S.J., Gibson, S.B., 2008. Oxidative stress induces autophagic cell death independent of apoptosis in transformed and cancer cells. Cell Death Differ. 15, 171–182.
Chen, Y.C., Lin-Shiau, S.Y., Lin, J.K., 1998. Involvement of reactive oxygen species and caspase 3 activation in arsenite-induced apoptosis. J. Cell. Physiol. 177, 324–333.
Cho, D.H., Jo, Y.K., Hwang, J.J., Lee, Y.M., Roh, S.A., Kim, J.C., 2009. Caspase-mediated cleavage of ATG6/Beclin-1 links apoptosis to autophagy in HeLa cells. Cancer Lett. 274, 95–100.
Chowdhury, R., Chatterjee, R., Giri, A.K., Mandal, C., Chaudhuri, K., 2010. Arsenic-induced cell proliferation is associated with enhanced ROS generation, Erk signaling and CyclinA expression. Toxicol. Lett. 198, 263–271.
D'Amelio, M., Sheng, M., Cecconi, F., 2012. Caspase-3 in the central nervous system: beyond apoptosis. Trends Neurosci. 35, 700–709.
Delnomdedieu, M., Basti, M.M., Otvos, J.D., Thomas, D.J., 1994. Reduction and binding of arsenate and dimethylarsinate by glutathione: a magnetic resonance study. Chem.-Biol. Interact. 90, 139–155.
Diaz-Villasenor, A., Sanchez-Soto, M.C., Cebrian, M.E., Ostrosky-Wegman, P., Hiriart, M., 2006. Sodium arsenite impairs insulin secretion and transcription in pancreatic beta-cells. Toxicol. Appl. Pharmacol. 214, 30–34.
Ding, Z., Wang, X., Schnackenberg, L., Khaidakov, M., Liu, S., Singla, S., Dai, Y., Mehta, J.L., 2013. Regulation of autophagy and apoptosis in response to ox-LDL in vascular smooth muscle cells, and the modulatory effects of the microRNA hsa-let-7 g. Int. J. Cardiol. 168, 1378–1385.
Djavaheri-Mergny, M., Maiuri, M.C., Kroemer, G., 2010. Cross talk between apoptosis and autophagy by caspase-mediated cleavage of Beclin 1. Oncogene 29, 1717–1719.
Dringen, R., Spiller, S., Neumann, S., Koehler, Y., 2016. Uptake, metabolic effects and toxicity of arsenate and arsenite in astrocytes. Neurochem. Res. 41, 465–475.
Druwe, I.L., Vaillancourt, R.R., 2010. Influence of arsenate and arsenite on signal transduction pathways: an update. Arch. Toxicol. 84, 585–596.
Eblin, K.E., Hau, A.M., Jensen, T.J., Futscher, B.W., Gandolfi, A.J., 2008. The role of reactive oxygen species in arsenite and monomethylarsonous acid-induced signal transduction in human bladder cells: acute studies. Toxicology 250, 47–54.
Francois, F., Godinho, M.J., Grimes, M.L., 2000. CREB is cleaved by caspases during neural cell apoptosis. FEBS Lett. 486, 281–284.
Gibson, S.B., 2010. A matter of balance between life and death: targeting reactive oxygen species (ROS)-induced autophagy for cancer therapy. Autophagy 6, 835–837.
Gozuacik, D., Kimchi, A., 2007. Autophagy and cell death. Curr. Top. Dev. Biol. 78, 217–245.
He, X.Q., Chen, R., Yang, P., Li, A.P., Zhou, J.W., Liu, Q.Z., 2007. Biphasic effect of arsenite on cell proliferation and apoptosis is associated with the activation of JNK and ERK1/2 in human embryo lung fibroblast cells. Toxicol. Appl. Pharmacol. 220, 18–24.
Hosseini-Sharifabad, A., Mohammadi-Eraghi, S., Tabrizian, K., Soodi, M., Khorshidahmad, T., Naghdi, N., Abdollahi, M., Beyer, C., Roghani, A., Sharifzadeh, M., 2011. Effects of training in the Morris water maze on the spatial learning acquisition and VAChT expression in male rats. Daru. J. Fac. Pharm., Tehran Univ. Med. Sci. 19, 166–172.
Hughes, M.F., Beck, B.D., Chen, Y., Lewis, A.S., Thomas, D.J., 2011. Arsenic exposure and toxicology: a historical perspective. Toxicol. Sci.: Off. J. Soc. Toxicol. 123, 305–332.
Jain, M.V., Paczulla, A.M., Klonisch, T., Dimgba, F.N., Rao, S.B., Roberg, K., Schweizer, F., Lengerke, C., Davoodpour, P., Palicharla, V.R., Maddika, S., Los, M., 2013. Interconnections between apoptotic, autophagic and necrotic pathways: implications for cancer therapy development. J. Cell. Mol. Med. 17, 12–29.
Jiang, S., Su, J., Yao, S., Zhang, Y., Cao, F., Wang, F., Wang, H., Li, J., Xi, S., 2014. Fluoride and arsenic exposure impairs learning and memory and decreases mGluR5 expression in the hippocampus and cortex in rats. PLoS One 9, e96041.
Jing, J., Zheng, G., Liu, M., Shen, X., Zhao, F., Wang, J., Zhang, J., Huang, G., Dai, P., Chen, Y., Chen, J., Luo, W., 2012. Changes in the synaptic structure of hippocampal neurons and impairment of spatial memory in a rat model caused by chronic arsenite exposure. Neurotoxicology 33, 1230–1238.
Kang, R., Zeh, H.J., Lotze, M.T., Tang, D., 2011. The Beclin 1 network regulates autophagy and apoptosis. Cell Death Differ. 18, 571–580.
Keim, A., Rossler, O.G., Rothhaar, T.L., Thiel, G., 2012. Arsenite-induced apoptosis of human neuroblastoma cells requires p53 but occurs independently of c-Jun. Neuroscience 206, 25–38.
Khorshidahmad, T., Tabrizian, K., Vakilzadeh, G., Nikbin, P., Moradi, S., Hosseini-Sharifabad, A., Roghani, A., Naghdi, N., Sharifzadeh, M., 2012. Interactive effects of a protein kinase AII inhibitor and testosterone on spatial learning in the Morris water maze. Behav. Brain. Res. 228, 432–439.
Komissarova, E.V., Saha, S.K., Rossman, T.G., 2005. Dead or dying: the importance of time in cytotoxicity assays using arsenite as an example. Toxicol. Appl. Pharmacol. 202, 99–107.
Kralova, V., Benesova, S., Cervinka, M., Rudolf, E., 2012. Selenite-induced apoptosis and autophagy in colon cancer cells. Toxicol. Vitr.: Int. J. Publ. Assoc. BIBRA 26, 258–268.
Lau, A., Whitman, S.A., Jaramillo, M.C., Zhang, D.D., 2013a. Arsenic-mediated activation of the Nrf2-Keap1 antioxidant pathway. J. Biochem. Mol. Toxicol. 27, 99–105.
Lau, A., Zheng, Y., Tao, S., Wang, H., Whitman, S.A., White, E., Zhang, D.D., 2013b. Arsenic inhibits autophagic flux, activating the Nrf2-Keap1 pathway in a p62-dependent manner. Mol. Cell. Biol. 33, 2436–2446.
Li, D., Ueta, E., Kimura, T., Yamamoto, T., Osaki, T., 2004. Reactive oxygen species (ROS) control the expression of Bcl-2 family proteins by regulating their phosphorylation and ubiquitination. Cancer Sci. 95, 644–650.
Luanpitpong, S., Chanvorachote, P., Stehlik, C., Tse, W., Callery, P.S., Wang, L., Rojanasakul, Y., 2013. Regulation of apoptosis by Bcl-2 cysteine oxidation in human lung epithelial cells. Mol. Biol. Cell 24, 858–869.
Luo, J.H., Qiu, Z.Q., Shu, W.Q., Zhang, Y.Y., Zhang, L., Chen, J.A., 2009. Effects of arsenic exposure from drinking water on spatial memory, ultra-structures and NMDAR gene expression of hippocampus in rats. Toxicol. Lett. 184, 121–125.
Luster, M.I., Simeonova, P.P., 2004. Arsenic and urinary bladder cell proliferation. Toxicol. Appl. Pharmacol. 198, 419–423.
Martinez-Finley, E.J., Ali, A.M., Allan, A.M., 2009. Learning deficits in C57BL/6J mice following perinatal arsenic exposure: consequence of lower corticosterone receptor levels? Pharmacol. Biochem. Behav. 94, 271–277.
Matsuzaki, K., Yamakuni, T., Hashimoto, M., Haque, A.M., Shido, O., Mimaki, Y., Sashida, Y., Ohizumi, Y., 2006. Nobiletin restoring beta-amyloid-impaired CREB phosphorylation rescues memory deterioration in Alzheimer's disease model rats. Neurosci. Lett. 400, 230–234.
Mizuno, M., Yamada, K., Maekawa, N., Saito, K., Seishima, M., Nabeshima, T., 2002. CREB phosphorylation as a molecular marker of memory processing in the hippocampus for spatial learning. Behav. Brain Res. 133, 135–141.
Mizushima, N., Yoshimori, T., 2007. How to interpret LC3 immunoblotting. Autophagy 3, 542–545.
Nassireslami, E., Nikbin, P., Amini, E., Payandemehr, B., Shaerzadeh, F., Khodagholi, F., Yazdi, B.B., Kebriaeezadeh, A., Taghizadeh, G., Sharifzadeh, M., 2016. How sodium arsenite improve amyloid beta-induced memory deficit? Physiol. Behav. 163, 97–106.
O'Bryant, S.E., Edwards, M., Menon, C.V., Gong, G., Barber, R., 2011. Long-term low-level arsenic exposure is associated with poorer neuropsychological functioning: a Project FRONTIER study. Int. J. Environ. Res. Public Health 8, 861–874.
Pattingre, S., Tassa, A., Qu, X., Garuti, R., Liang, X.H., Mizushima, N., Packer, M., Schneider, M.D., Levine, B., 2005. Bcl-2 antiapoptotic proteins inhibit Beclin 1-dependent autophagy. Cell 122, 927–939.
Qian, W., Liu, J., Jin, J., Ni, W., Xu, W., 2007. Arsenic trioxide induces not only apoptosis but also autophagic cell death in leukemia cell lines via up-regulation of Beclin-1. Leuk. Res. 31, 329–339.
Ratnaike, R.N., 2003. Acute and chronic arsenic toxicity. Postgrad. Med. J. 79, 391–396.
Rodriguez, V.M., Carrizales, L., Jimenez-Capdeville, M.E., Dufour, L., Giordano, M., 2001. The effects of sodium arsenite exposure on behavioral parameters in the rat. Brain Res. Bull. 55, 301–308.
Rodriguez, V.M., Jimenez-Capdeville, M.E., Giordano, M., 2003. The effects of arsenic exposure on the nervous system. Toxicol. Lett. 145, 1–18.
Salminen, A., Kaarniranta, K., Kauppinen, A., 2013. Beclin 1 interactome controls the crosstalk between apoptosis, autophagy and inflammasome activation: impact on the aging process. Ageing Res. Rev. 12, 520–534.
Scherz-Shouval, R., Shvets, E., Elazar, Z., 2007. Oxidation as a post-translational modification that regulates autophagy. Autophagy 3, 371–373.
Sharifzadeh, M., Sharifzadeh, K., Naghdi, N., Ghahremani, M.H., Roghani, A., 2005. Posttraining intrahippocampal infusion of a protein kinase AII inhibitor impairs spatial memory retention in rats. J. Neurosci Res. 79, 392–400.
Shin, S.Y., Hyun, J., Yu, J.R., Lim, Y., Lee, Y.H., 2011. 5-Methoxyflavanone induces cell cycle arrest at the G2/M phase, apoptosis and autophagy in HCT116 human colon cancer cells. Toxicol. Appl. Pharmacol. 254, 288–298.
Simeonova, P.P., Wang, S., Toriuma, W., Kommineni, V., Matheson, J., Unimye, N., Kayama, F., Harki, D., Ding, M., Vallyathan, V., Luster, M.I., 2000. Arsenic mediates cell proliferation and gene expression in the bladder epithelium: association with activating protein-1 transactivation. Cancer Res. 60, 3445–3453.
Taghizadeh, G., Pourahmad, J., Mehdizadeh, H., Foroumadi, A., Torkaman-Boutorabi, A., Hassani, S., Naserzadeh, P., Shariatmadari, R., Gholami, M., Rouini, M.R., Sharifzadeh, M., 2016. Protective effects of physical exercise on MDMA-induced cognitive and mitochondrial impairment. Free Radic. Biol. Med. 99, 11–19.
Thorburn, A., 2008. Apoptosis and autophagy: regulatory connections between two supposedly different processes. Apoptosis: Int. J. Program. Cell Death 13, 1–9.
Trejo-Solís, C., Jimenez-Farfan, D., Rodriguez-Enriquez, S., Fernandez-Valverde, F., Cruz-Salgado, A., Ruiz-Azuara, L., Sotelo, J., 2012. Copper compound induces autophagy and apoptosis of glioma cells by reactive oxygen species and jnk activation. BMC Cancer 12, 156.
Tsai, S.Y., Chou, H.Y., The, H.W., Chen, C.M., Chen, C.J., 2003. The effects of chronic arsenic exposure from drinking water on the neurobehavioral development in adolescence. Neurotoxicology 24, 747–753.
Vahter, M., 1981. Biotransformation of trivalent and pentavalent inorganic arsenic in mice and rats. Environ. Res. 25, 286–293.

Watcharasit, P., Visitnonthachai, D., Suntararuks, S., Thiantanawat, A., Satayavivad, J., 2012. Low arsenite concentrations induce cell proliferation via activation of VEGF signaling in human neuroblastoma SH-SY5Y cells. Environ. Toxicol. Pharmacol. 33, 53–59.

Williams, C.M., El Mohsen, M.A., Vauzour, D., Rendeiro, C., Butler, L.T., Ellis, J.A., Whiteman, M., Spencer, J.P.E., 2008. Blueberry-induced changes in spatial working memory correlate with changes in hippocampal CREB phosphorylation and brain-derived neurotrophic factor (BDNF) levels. Free Radic. Biol. Med. 45, 295–305.

Wirawan, E., Vande Walle, L., Kersse, K., Cornelis, S., Claerhout, S., Vanoverberghe, I., Roelandt, R., De Rycke, R., Verspurten, J., Declercq, W., Agostinis, P., Vanden Berghe, T., Lippens, S., Vandenabeele, P., 2010. Caspase-mediated cleavage of Beclin-1 inactivates Beclin-1-induced autophagy and enhances apoptosis by promoting the release of proapoptotic factors from mitochondria. Cell Death Dis. 1, e18.

Yang, P., He, X.Q., Peng, L., Li, A.P., Wang, X.R., Zhou, J.W., Liu, Q.Z., 2007. The role of oxidative stress in hormesis induced by sodium arsenite in human embryo lung fibroblast (HELF) cellular proliferation model. J. Toxicol. Environ. Health Part A 70, 976–983.

Yousefi, S., Simon, H.U., 2007. Apoptosis regulation by autophagy gene 5. Crit. Rev. Oncol./Hematol. 63, 241–244.

Yue, Z., Friedman, L., Komatsu, M., Tanaka, K., 2009. The cellular pathways of neuronal autophagy and their implication in neurodegenerative diseases. Biochim. Biophys. Acta 1793, 1496–1507.